TECHNOLOGY AND EQUIPMENT FOR PLASMA SURFACE HARDENING OF HEAVY-DUTY PARTS

S.V.Petrov and A.G.Saakov

ABSTRACT

Local heat treatment is justifiable in many cases in terms of technology and cost effectiveness, where only the most loaded working surface is subjected to hardening, while the bulk of a material remains untreated. Plasma surface hardening allows wear to be decreased and service life of heavy-loaded machine parts to be extended 2-5 times. The novel method of plasma hardening is technically and economically preferable for heat treatment of a large number of parts. One example of its application is high-speed surface hardening of all types of passenger, freight and locomotive train wheelsets. Tests show that in all cases the amount of wear of the wheelset ridges after plasma hardening is much lower (2.5-3.0 times) than that of the ridges after standard heat treatment.

1.0 Introduction

Among other technologies for surface engineering, the process of plasma surface hardening is gaining an increasingly wide acceptance. This process uses a multicomponent reactive plasma of products of combustion of hydrocarbon gases with air. It is characterized by a combination of unique transport and thermal-physical properties. From the technology standpoint, this includes the easy-to-control oxidation-reduction potential, the ability of effectively heating and accelerating dispersed materials and controlling parameters of the stabilized electric-arc discharge, etc. These are the key properties, which motivated development of a new science-and-technology area and made the use of this plasma especially attractive for technologies of plasma and electric-arc spraying and treatment of materials. The involved plasma gases, being affordable and inexpensive, are the gases of choice in modern engineering characterized by increasing capacities of machines and, accordingly, productivity of processes, where working parameters shift toward increased gas flow rates.

The new approach to making machines for high-speed plasma surface hardening has been developed based on utilization of the variable-composition mixture of gas and air and the stabilized elongated electric arc that burns in a plasmatron and is adapted to meet the technology requirements.

2.0 Process equipment

Milestones in improvement of equipment are associated primarily with development and realization of new approaches, and in recent years with using measurement and control digital devices. Based on the above ideology, RPE TOPAS Ltd. developed and started up manufacture of a number of new high-tech plasma machines to implement new technologies.

To realize this idea, the Company developed plasmatrons designed for different power levels, as well as hardware for high-speed surface hardening of various parts. The plasmatrons are

based on a new approach to formation of the extended plasma jet. A decreased dissipation of jet power is ensured by suppression of turbulence in the boundary layer. This is achieved by making use of the fine effects of dynamics of the plasma. Main peculiarities of behavior of the molecular gas plasma under non-equilibrium conditions are associated with oscillatory-translational non-equilibrium, which might amount to several thousands of degrees. In this situation the probability exists of reversion of the effect of the second viscosity (the second or bulk viscosity becomes negative). This leads to build-up of the sound generated by the natural turbulence, rather than to its attenuation. The efficient reinforcement of the sound due to reversion of the second viscosity occurs at frequencies of 10-100 kHz. The intensive sound waves, which are formed and reinforced in one region of the flow and absorbed in the other (downstream), can have a considerable effect on hydrodynamic parameters of the flow and electrophysical properties of the discharge. The plasma jet generated in this case is characterized by increased (by 30 %) accelerating and heating capabilities.

The set of equipment for plasma hardening includes:

1. High-speed surface hardening machine UVPZ-2M (Fig. 1), which comprises:
- power supply (Plasma-TOPAS) 1 pc.
- control devices 1 set
  - control unit
  - computer unit
  - arc ignition unit
  - gas unit
- plasma modules 2 sets
  - plasmatron
  - heating module
  - "TOPAS-Smotrich" pyrometer
  - communication

If necessary, the machine can be equipped with a unit for independent cooling with a closed water feed cycle.

Specifications

Installed power of the machine, kVA	105
Power of the plasmatron, kW	60
Mains voltage, 3 phase, A.C., 50 Hz, V	380
Flow rate of compressed air at pressure in the supply system equal to 0.5-0.6 MPa, m^3/h	5-8
Fuel gas flow rate, m^3/h:	
methane	0.5
propane-butane	0.2
Cooling water consumption at pressure in the supply system equal to 0.3 MPa, m^3/h	1.5
Duty cycle, %	100
Depth of the hardened zone, mm	2.5-3.5
Width of the hardened zone, mm	25-35

2. A semi-automatic line for hardening of wheelsets with wheeling out (Fig. 2), which comprises:
- noise- and radiation-proof chamber 1 set

- device for transportation of wheelsets	1 set
- control devices	1 set

Specifications

Conveyer speed, m/min	8.2
Wheelset rotation speed, rpm	0.25
Productivity of the line, wheelset/hour	4

The UVPZ-2M machine is equipped with an independent optimization unit to provide:
- in-process programming of conditions and parameters, indication of the current condition of the controlled process parameters, recording and storing of parameters of the process of plasma surface hardening of wheelsets in permanent memory and output of the information accumulated to a personal computer;
- processing of analogue signals from the "TOPAS-Smotrich" pyrometer, the "Plasma-TOPAS" plasmatron power supply and pressure sensors, as well as input discrete signals from the final control mechanisms and formation of output commands for programmed control.

The front panel of the digital indication unit includes a keyboard and a two-row indicator for reading of the current values of parameters, time and in-process condition information.

3.0 Modeling of the plasma hardening process

The key task of the mathematical support in the form of the specialized software package based on modern computer facilities is to optimize the hardening process through selection of heating-cooling conditions which would provide the desirable strength properties for a given material (steel grade) within the preset area of heat treatment.

Fulfilment of this task is associated with a possibility of having a reliable prediction of the material structure to be produced, based on the selected thermal effect parameters. Considering complexity of the latter, the development of the software was divided into three inter-related and, at the same time, sufficiently independent stages.

Stage 1 involved solution of the problem associated with computation of thermal cycles for an arbitrary micro-volume within the treatment area for the preset type of material. Density of a material, as well as temperature dependence of thermal conductivity and specific heat are considered to be known [1]. External effects which can vary over a wide range include consumption, initial temperature and thermal-physical properties of the plasma, size of the zone to be heated, character of relative displacement, speed of displacement of the material treated, degree of preheating-cooling, cooling conditions upon leaving the plasma treatment zone, etc.

It should be noted, however, that the latter approach is associated with many preliminary experimental studies, while reliability of the results obtained dramatically decreases even with a slight deviation of parameters outside the range studied.

Optimization of the technology involves special precautions to produce the preset configuration of the plasma flow and the proper selection of required conditions of the hardening process. Reliable prediction of structures and residual stresses formed in the hardened layer can be made only in the case of using a non-linear mathematical model.

Allowance for non-linearity of thermal-physical parameters of the plasma and material treated makes it possible to determine local extreme of rates of variations in temperature of certain micro-volumes within certain time intervals.

Further increase in level of service properties of a part being hardened can be achieved through improvement of the hardening technology, which is eventually reduced to ensuring the optimal thermal cycle (heating-cooling), proceeding from regularities in structural, phase and polymorphic transformations of the material hardened.

Stage 2 involved development of the software for modeling the processes of structural, physical and chemical transformations occurring in the material studied, under substantially non-equilibrium conditions of rapid heating and cooling, proceeding from the fundamental up-to-date concepts of the processes being investigated. In principle, occurrence of these processes and variations in thermal conditions of the material treated are a single process. Thus, they should be computed simultaneously, because structural, phase and chemical transformations are related in this or that way to absorption or release of latent heat. However, the available reliable literature data on thermal-physical properties of the material treated implicitly make allowance for the above processes (e.g. the data on specific heat include values of the effective apparent heat capacity, and the same applies to thermal conductivity). In addition, under the considered conditions of rapid heating and cooling the diffusion processes substantially lag behind the thermal ones. Therefore, the above separation of the procedures of computation of thermograms and transformations in the material treated seems justifiable.

Difficulties in stage 2 are associated firstly with the absence of a common opinion concerning the process of formation of austenite during heating and its decomposition during cooling. Secondly, in the majority of the available literature sources describing the hardening processes for certain classes of materials, the data given are in the best case the result of mathematical processing (plots, tables) of experimental studies. As a rule it is very difficult to get from them the information concerning mechanisms of the processes occurring and quantitative estimates of the processes taking place in an individual micro-volume, which are important for description.

For this paper the authors selected as a reference point a relatively small number of works, where all variations taking place in micro-volumes are described on the basis of fundamental concepts of the material and energy conversion processes.

The problem of modeling of the heat treatment process consists in computation of the quantity of austenite formed during the period of heating (in compliance with the thermogram plotted for a given micro-volume) and, accordingly, the percentage of that quantity of austenite which remains non-decomposed at the moment of achieving the martensitic transformation temperature at a stage of cooling.

Mathematical description of these transformation processes is based on the diffusion equation of the form:

$$\partial C/\partial \tau = \partial[D(t)\cdot\partial C/\partial x]/\partial x,$$

where C is the carbon concentration, D(t) is the carbon diffusion coefficient depending upon the temperature t, x is the space coordinate, τ is the time recorded for each of the micro-volume structures allowing for their boundary conditions.

The latter depend upon the type of steel considered, whether it is hypoeutectoid (containing ferrite and pearlite), eutectoid (containing only pearlite) or hypereutectoid (containing pearlite and cementite). In this case the conditions for free ferrite and ferrite which is part of pearlite are different. This is equally true for cementite. In addition, the type of the boundary conditions greatly depends upon the a priori simplified assumptions of the morphological peculiarities of individual structural elements of the micro-volume.

As an example, consider the case of hardening of eutectoid steel following the preset thermogram:

$$t=t(\tau), \qquad 0\le\tau\le T$$

where T is the total hardening time. In this case τ_1 is the moment of achieving the martensitic transformation temperature at the stage of heating, τ_2 is the moment of achieving a temperature of 727 °C at the stage of heating, τ_3 is the moment of achieving a temperature of 727 °C at the stage of cooling and τ_4 is the moment of achieving the martensitic transformation temperature at the stage of cooling:

$$T\ge\tau_1 + \tau_2 + \tau_3 +\tau_4$$

For the process of formation of austenite as a result of decomposition of cementite of the pearlite grain ($\alpha-\gamma$ transition), the following boundary and initial conditions ($\tau_2 < \tau \le\tau_3$) are valid.

At the cementite-austenite boundary

$$C(\tau,\xi_1) = C_{max}(t),\ D(t)\cdot\partial C/\partial x|x =\xi_1= (0{,}0667-C_{max}(t))\cdot d\xi_1/d\tau,\ \ 0\le x\le\xi_1$$

and at the austenite-ferrite boundary

$$C(\tau,\xi_2)=C_{min}(t),\ \ D(t)\cdot\partial C/\partial x|x=\xi_2 = (0{,}0002-C_{min}(t))\cdot d\xi_2/d\tau,\ \ \xi_1\le x\le\xi_2\le\xi_{2max}$$

$$\xi_1(\tau_2) = 0.5\cdot\delta Ce(\tau 2);\ \ \xi_2(\tau_2) = 0.5\cdot\delta Ce(\tau_2) + \delta A(\tau_2);$$

$$\xi_{2max} = 0.5\cdot(\delta F+\delta Ce+ \delta A)$$

Here:
$C_{min}(t)$ is the equilibrium carbon concentration in austenite at the boundary with ferrite (GS curve in the constitution diagram);
$C_{max}(t)$ is the equilibrium carbon concentration in austenite at the boundary with cementite (SE curve in the constitution diagram);
ξ_1 is the austenite-cementite boundary coordinate;
ξ_2 is the austenite-cementite boundary coordinate;
D(t) is the coefficient of diffusion of carbon into austenite;

δF, δCe, δA, $\delta F(\tau)$, $\delta Ce(\tau)$, $\delta A(\tau)$ are the thicknesses of the ferrite, cementite and austenite layers within the pearlite zone at the initial moment ($\tau=0$) and arbitrary moment τ, respectively;
δA is determined from the value of the initial martensite content of steel.

For the stage of decomposition of austenite within the $\tau_1 < \tau \leq \tau_2$ and $\tau_3 < \tau \leq \tau_4$ ranges, it holds that:
at the cementite-austenite boundary:

$$C(\tau,\xi_1) = C^*_{max}(t),\ D(t)\cdot\partial C/\partial x|x = \xi_1 = (0{,}0667 - C^*_{max}(t)) - d\xi_1/d\tau,\ 0 \leq x \leq \xi_1$$

at the austenite-ferrite boundary:

$$C(\tau,\xi_2) = C^*_{min}(t),\ D(t)\cdot\partial C/\partial x|x = \xi_2 = (0{,}0002 - C^*_{min}(t)) - d\xi_2/d\tau,$$

$$\xi_1 \leq x \leq \xi_2 \leq \xi_{2max},\ \xi_1(\tau_1) = 0.5\cdot\delta Ce;\ \xi_2(\tau_1) = 0.5\cdot\delta Ce + \delta A;$$

where $C^*_{max}(t)$ and $C^*_{min}(t)$ are the continuations of the SE and GS curves into the range of temperatures below 727 °C, respectively.

Problems of stage 3 concerning development of the software, associated with construction of correlation models of the type of "material structure - physical-mechanical properties" are not considered within this paper.

4.0 Experimental Procedure

Plasma of the products of combustion of air with a hydrocarbon fuel gas was used for surface heat treatment [2]. Car and locomotive wheelsets were subjected to hardening using the UVPZ-2M machine.

Test pieces were cut from the heat treated wheel surface using a diamond tool. High-speed heat treatment, in particular plasma surface hardening, results in the formation of the dispersed phase transformation products which are
localized in thin metal layers.

The thin cold-worked layer formed on the test piece surface as a result of mechanical polishing was removed in order to reveal and correctly interpret structural components. For this the test pieces were subjected to electrolytic polishing in a chrome-acetic electrolyte, and then to etching in a weak solution of nitric acid and a reagent of the composition: 20 % oxalic acid solution with an addition of a few drops of sulphuric acid. The etching conditions were as follows: voltage - 20 V, time - 10-15 s. Chemical composition of steel investigated was as follows: C - 0.50-0.60 %, Mn - 0.60-0.90 %, Si - 0.20-0.42 %, P < 0.035 %, S < 0.04 %, balance - Fe.

The test pieces were investigated using the JSM-840 scanning electron microscope equipped with the Link 860/500 microanalysis system (Great Britain). X-ray diffraction analysis was done using the DRON-2,0 X-ray diffractometer with copper monochromatic radiation.

Microhardness of the test pieces was measured using the "LECO" microhardness tester under a load of 50 g on the indentor at a pitch of 0.1 mm. Averaging was done over 20

measurements. The "Slide" software program for the IBM-compatible computers was used to generalize the results of microhardness measurements. Microstructure and microhardness were investigated through thickness of the treated layer to the base metal. Variations in microstructure confirmed the data of the microhardness measurements. Electron microscopy and light microscopy showed the following [3]. Structure of the base metal is primarily a mixture of ferrite and pearlite with precipitates of ferritic rings along the grain boundaries, having microhardness of 285 N/mm^2 under a load of 200 g on the indentor.

Interlayers of hypoeutectoid ferrite are 2-3 μm thick and have a smooth defect-free (slightly etched out) surface. Pearlite colonies are equiaxed, having a mean diameter of 5-15 μm, the lamina spacing being about 0.15 μm.

In the heat-affected zone no marked changes in morphology of pearlite were detected. However, hardness was somewhat higher and corresponded to 305 N/mm^2. In the intercritical range (ICR) adjoining the base metal (near A_{C1}), inside the pearlite colonies, the nuclei of austenite started forming, which were then transformed into martensite during subsequent cooling. This martensite is very fine. Towards the surface, an acicular structure of upper bainite and structureless martensite are formed. Microhardness of structureless martensite varies from 380 N/mm^2 near the surface to 350 N/mm^2 at a distance of 1500 μm from the surface. In the upper part of the intercritical range martensite occupies the larger part of the metal volume (more than 60 %) and the pearlite colonies are split into individual islands not related to each other.

In some cases, remainders of the undissolved cementite laminae were found in martensite. This is attributable to a short time during which the metal dwells in the intercritical range. They show up as hard-to-detect threads, which are the initial laminae of cementite of undissolved pearlite that continue into martensite.

At a depth of about 0.9-1.0 mm, martensite dominates in the metal structure (above 70 %), while the remainders of the undissolved cementite laminae and hypoeutectoid ferrite are found in rare cases. From the surface to a depth of about 0.5 mm, under rigid conditions the heat treated layer becomes fully martensitic, although still dispersed. However, in some locations the acicular (laminated) structure of martensite is clearly defined. This is likely to be assisted by some increase in size of the pearlite grain, caused by increased temperatures of the subsurface layer. Microhardness of the layer through its entire thickness (0-0.9 mm) is 450-390 N/mm^2. Typical distribution of microstructures and hardness through thickness of the hardened zone is shown in Fig. 3.

With X-ray diffraction analysis of symmetry and structure of the interference maximum (200) was done using the known methods to identify the type of structure in the hardened layer. The interference profile (200) from the surface of the test piece taken from the wheel rim after plasma treatment (Fig.4a) and two reference test pieces taken from the wheel steel of the identical chemical composition after martensite quenching from a temperature of 860 °C (holding for 20 min) (Fig.4b) and after annealing at a temperature of 680 °C for 5 hours (Fig.4c) was recorded within the Wolf-Bragg angle range of 20-60-70 degrees using the DRON-2,0 X-ray diffractometer with copper monochromatic radiation.

The interference profile (200) obtained on a test piece subjected to plasma treatment is characterized by a high symmetry (Fig. 4a). Interference (200) of the hardened test piece is asymmetrical about the main maximum, and on the side of small values of the Wolf-Bragg

angles it has a second peak of a lower intensity, specified by an arrow (Fig.4b). This doubling of interference (200), as well as of other interferences, is typical for structures of the martensitic type. It is due to tetragonality of the martensite lattice caused by ordering of the carbon atoms in octahedral positions of the γ-iron lattice. Doubling of interferences in the diffraction patterns is observed at a high carbon content (0.4-0.6 %) of the γ-iron lattice. At a lower degree of oversaturation of γ-iron with carbon (0.20-0.35 %) the interference peaks can have a marked asymmetry (gradual growth to a maximum value) only on the side of small values of the Wolf-Bragg angles. Structures with this type of interference maxima are classified as "tempered martensite".

Therefore, as established by optical and electron microscopy, as well as X-ray diffraction analysis, the structure of the hardened layer is a highly dispersed mixture which contains primarily low-carbon tempered martensite, a small amount of high carbon martensite and some amount of undissolved cementite (carbides). This conglomerate of structures is attributable to the fact that heating in plasma hardening amounts to very high temperatures and takes a very short time. Therefore, the processes of growth of the austenite grain, its homogenization and full dissolution of cementite have no time to be completed.

Measurements of microhardness through the entire thickness, i.e. from the surface to the base metal, show the following. Between the zone of complete recrystallization and that of ICR there occurs a dramatic decrease to 35 N/mm^2 in microhardness. Starting approximately from the centre of ICR and up to the heat-affected zone, microhardness increases by 30 N/mm^2 on the average. In the heat-affected zone there is a gradual decrease in microhardness until the base metal is reached, where it becomes stabilized. There is a microhardness dip, which can be shifted to a certain degree and is located between the heat-affected zone and the base metal.

Different researchers observed the microhardness dip in the transition layer between the martensite structure and the basic structure in the centre, which is formed during the process of heat hardening by the method of interrupted quenching. Increased tensile stresses are formed in this location. In our case such stresses can be formed also during phase recrystallization.

Generalization of the accumulated experience in operation of wheelsets is indicative of the fact that there are certain specific features in their damages and in structure of defects of metal which determine these damages. The above factors have a direct effect on safe and efficient operation of wheelsets.

Mechanism of initiation of microcracks in high-temperature surface hardening of shrouds of locomotive wheelsets was studied. In the unfavourable situation these microcracks may lead to fracture. A similar situation occurs in heating of the roll surface of a wheel by brake blocks in the case of emergency braking. This is a new and vast area, which cannot be covered in a short article. However, it makes sense to give here the main result of the studies. Understanding of the mechanism of formation of dangerous microcracks and fracture of a complex-loaded part with a sufficiently high safety factor resulted from direct transmission examinations of fine structure of the heat-treated surface layer of metal. Studies were conducted using the JEM-2000CX instrument (Jeol Company) at an accelerating voltage of 200 kV. Foils for electron microcopy were made by electric-spark cutting, followed by mechanical thinning using abrasive cloth, electrolytic polishing and finish ion thinning. Direct electron microscopy of structure-phase composition of the subsurface layer metal in a

location of transition from the hardened zone to the base metal (point * in Fig. 3) is illustrated in Fig. 5. Fig. 5 a shows the equilibrium fine structure with fine-lamina cementite formations 0.005-0.5 μm thick. Internal fine structure of ferritic rings is sufficiently compensated for and characterized by uniform distribution of dislocations. The intergranular zone (contact of hard and soft structural components) has no gradients of dislocation density. No clustering or presence of internal stress raisers is revealed. Under the unfavourable thermomechanical effect, at the same point * shown in Fig. 3, fine structure of the subsurface layer has the form shown in Fig. 5b. Cementite laminae change orientation from linear (Fig. 5 a) to vortex-type (Fig. 5b). Degradation and violation of a monolithic character are clearly seen. Metal structure in the above zone has all signs of considerable internal stresses. As a rule, formation and propagation of microcracks take place in the ferrite regions adjoining the pearlite ones.

5.0 Results and Discussion

Heat hardening of steel parts is one of the most efficient and effective methods for extension of service life of heavy-loaded parts of machines and mechanisms and for decreasing their wear. In many cases only local treatment is justifiable technically and economically. In this case hardening is done only to the most loaded working surface of a part, whereas the central part remains untreated. High-frequency and flame heat treatment gained the widest industrial acceptance for surface hardening of parts. Further advances in quality of heat treatment of working surfaces of parts are associated with the use of concentrated energy sources, such as electron and laser beams and plasma jets. The use of these sources provides improved quality of hardening and better performance of parts. The plasma method is the most cost effective and productive among other methods of heat treatment involving concentrated heat sources. This method is characterized by reduced costs, higher affordability of the process equipment and larger sizes of the hardened zone.

The technology of plasma surface hardening of TOPAS Ltd. is characterized by new capabilities in terms of increasing contact-fatigue strength and, therefore, increasing reliability of traction for locomotive wheelsets [4]. Intensity of wear of the wheelset ridges after plasma hardening is much lower than that of the traditionally treated ones (2.5-3 times). The developed technology for hardening of the wheelsets has two peculiar features: 1.local (within the zone of the highest wear) surface hardening of the wheel ridge to a depth of 2.5-3 mm and width of 35 mm, ensuring an increase in hardness from 280 HB (in the base metal) to 450 HB. This provides an optimal relationship in hardness of the wheel and rail surfaces in contact; 2) change in structure of the hardened wheel zone from a ferrite-pearlite mixture with initial grain size of 30-40 μm to a mixture of fine-acicular or structureless martensite with a rosette-type troostite in a ratio of 50:50 %. This produces improvement of mechanical properties (including decrease in friction coefficient in contact of the ridge and the side surface of the rail) and increase in crack resistance of the wheel material within the plasma hardening zone.

Locomotives with the wheels plasma hardened by the TOPAS technology were first put into experimental operation at the Lviv-Zapad shed early in March 1996, and the cars - at the Kyiv-Passenger shed in summer that same year. Comparison of the plasma hardened wheel ridges of electric locomotives with the traditional ones under the same service conditions of the Lviv railway proved by the end of April 1996 the expected two-fold decrease in rate of wear. After that a decision was made to expand the scopes of application of plasma hardening of the wheelset ridges. It was for that purpose that the new specialized two-module high-speed plasma hardening machine UVPZ-2M was developed. Its application initiated the

arrangement of workshops for plasma hardening of wheelsets without wheeling out from under a locomotive, which was completed in 1997. This was done using the KZh-20 machine tool at the Znamenka shed. Similar workshops for plasma hardening with wheeling out were arranged in Osnova, Kharkiv. Workshops for plasma hardening of the wheelset ridges without wheeling out, based on the KZh-20 machine tool, were built at the Kazatin shed, those based on the K-40 machine tool were built at the Lviv-Zapad, Osnova (Kharkiv), Kotovsk, Nizhnedneprovsky junction, etc. (Fig. 6). The car wheels are hardened using the specialized production line with wheeling out at Kyiv, Kherson, Dneprodzerzhinsk and other car sheds.

The final outcome of more than 4 years operation of locomotives and cars with the plasma hardened wheelset ridges is as follows. 1.Plasma hardening is a highly productive efficient method for 2- or 3-fold extension of service life of the wheelsets, which can be applied under conditions of a typical car shed. The accepted technology provides a very high safety factor for operational reliability of the wheelsets. 2. The guaranteed reproducibility of the best indicators of operational reliability, and wear resistance is ensured by keeping precisely to the prescribed hardening parameters for every wheel.

6.0 Conclusions

1. The readily available high-enthalpy reactive air-gas plasma is widely applied as the plasma-forming environment for technology purposes. Theoretical principles of development of the high-efficiency equipment and technological processes that use it are described.

2. A new approach to making the plasma surface hardening machines is presented. New types of plasma hardware were developed, and new technological processes of high-speed plasma surface hardening were devised.

7.0 Acknowledgement

This work is done on order of the Ukrainian and Latvian railways. The authors are grateful to Mr. Lashko A.D., Deputy Director General of Ukrzaliznytsya, and Mr. N.I.Sergienko, Head of the Locomotive Facility Administration of Ukrzaliznytsya, for their consideration and cooperation in this work.

8.0 References

1. Petrov S.V., Saakov A.G. Plasma Surface Hardening of Wheelsets, Proceedings of the Eleventh International Conference on Surface Modification Technologies held in Paris, France, September 8-10, 1997. 516-525.
2. Petrov S.V., Saakov A.G. Combustion products plasma in surface engineering, TOPAS: Kiev, 2000; 265 p.
3. Petrov S.V., Saakov A.G. Microstructural Peculiarities of the Steel Surface Layers Treated with a Plasma. Advances in Special Electrometallurgy 1998, 1, 74-80.
4. Petrov S.V., Saakov A.G. Plasma High Velocity Hardening of Wheelsets, Proceedings of the 4th International Conference on Railway Bogies and Running Gears. Budapest, Hungary, 21-23 September, 1998, 453-462.

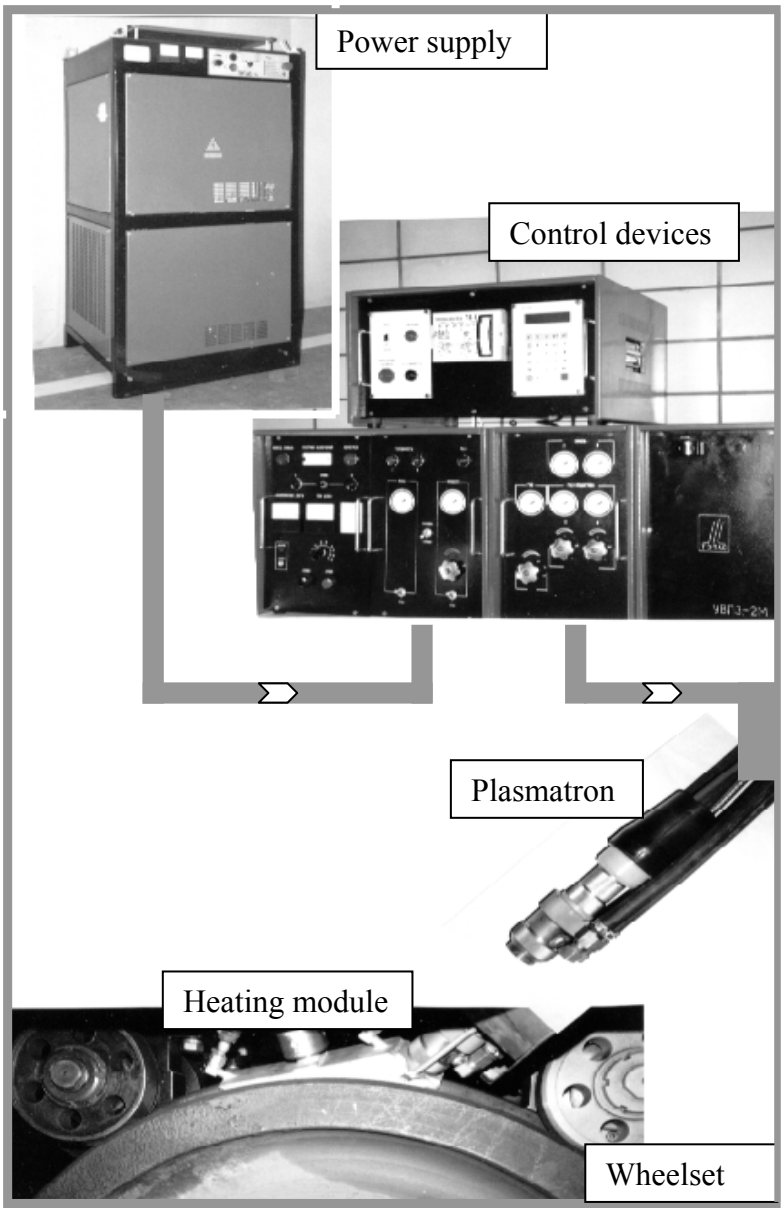

Fig. 1. High-speed surface hardening machine UVPZ-2M

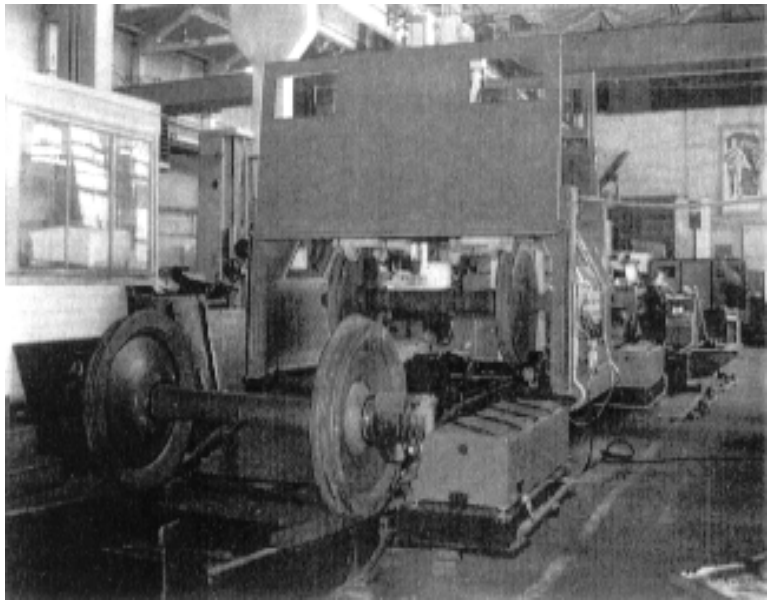

Fig. 2. A semi-automatic line for hardening of wheelsets with wheeling out

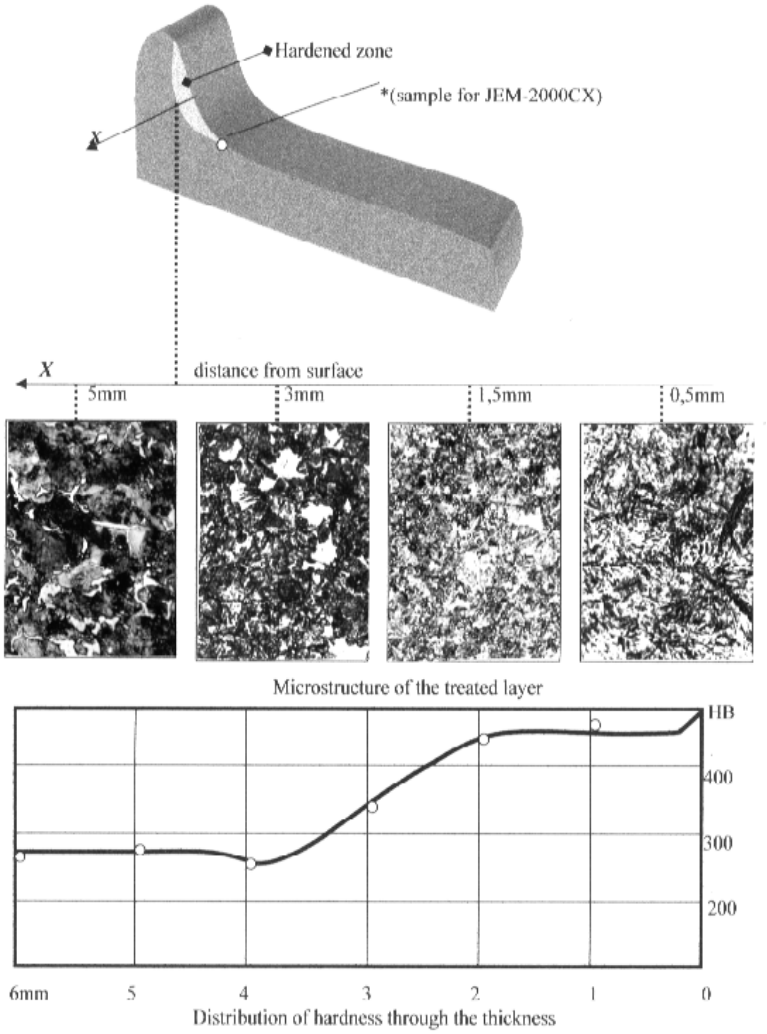

Fig. 3. Distribution of microstructures and hardness through thickness of the hardened zone

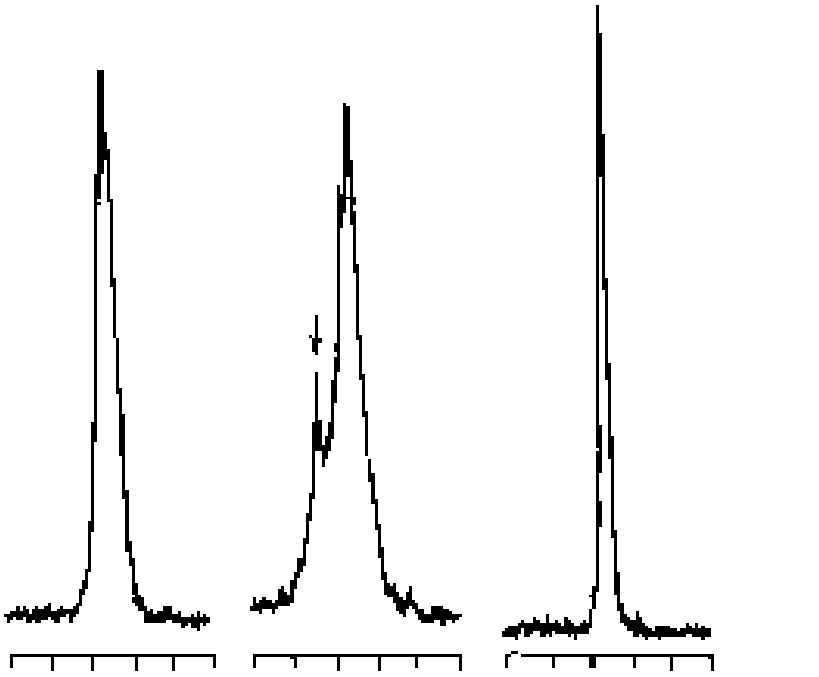

Fig.4. The interference profile (200) from the wheel rim
a--after plasma treatment; b--after martensite quenching; c--after annealing

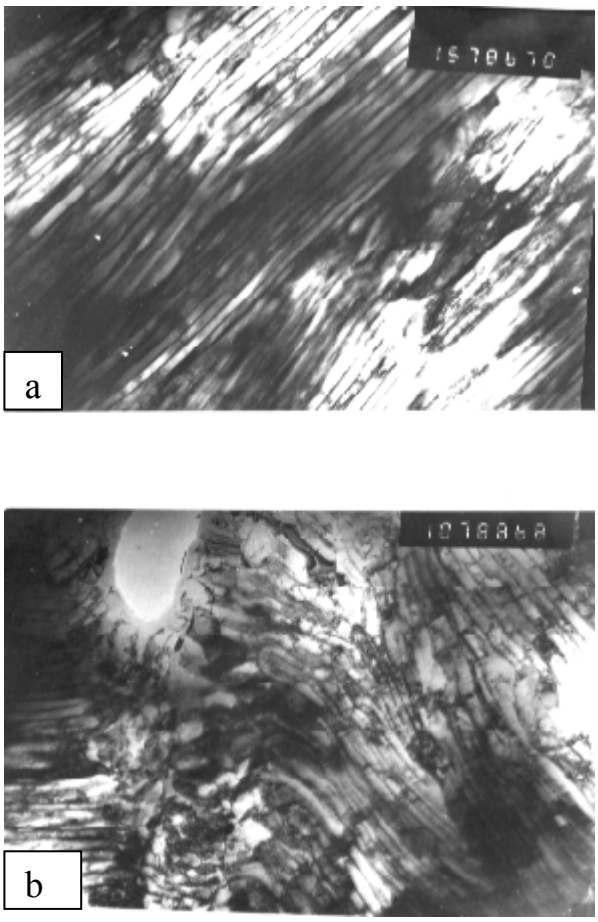

Fig.5. Structure-phase composition of the subsurface layer metal in a location of transition from the hardened zone to the base metal.
a--the equilibrium fine structure; b--the vortex-type structure

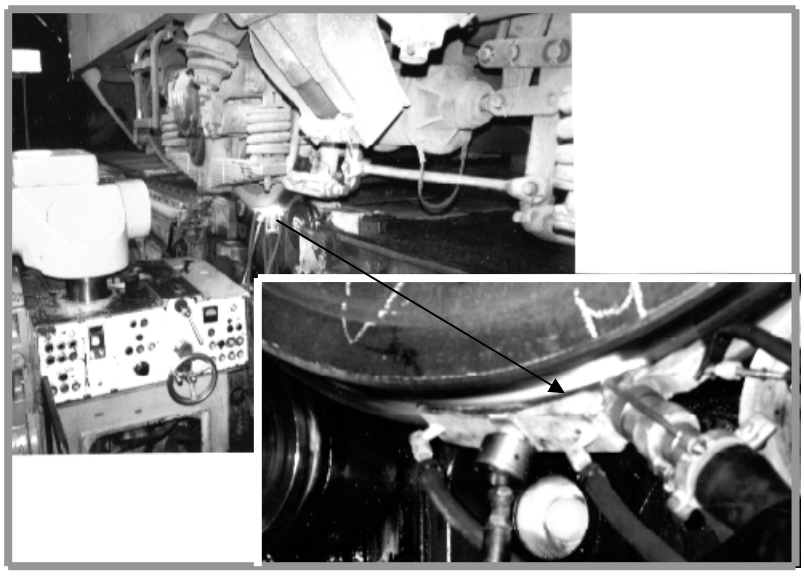

Fig.6. Plasma hardening of wheelsets without wheeling out from under a locomotive